Proceeding of the IEEE
International Conference on Robotics and Biomimetics
Dali, China, December 2019

Dynamic Height Balance Control for Bipedal Wheeled Robot Based on ROS-Gazebo

Tangyou Liu[1], Chao Zhang[1], Shuang Song[1]*, Max Q.-H. Meng[2], *Fellow, IEEE*

***Abstract*—In complex living environments, the application of mobile robots places higher demands on speed, flexibility, and affinity for people. This is an ongoing challenge in mobile robotics. Having these properties is an important research task for mobile robots in human settlements. The SR600 robot is a bipedal wheeled robot platform, developed by the RP laboratory of Harbin Institute of Technology, Shenzhen, is a human-like bipedal legged-wheeled robot. This paper introduces a method to realize changing height while the bipedal wheeled robot maintains dynamic balance, and simulated it by constructing a simple ROS-Gazebo simulation environment. Finally, the feasibility of the method is verified by a simple prototype experiment.**

***Index Terms*—bipedal legged-wheeled robot ; variable height dynamic balance control; ROS-Gazebo.**

I. Introduction

At present, there are many robots with two legs or two wheels, and have achieved good research results in both structure design and control methods. The biped robot Atlas of American Boston Dynamics can walk, run and even jump[1], [2]. *ASIMO* of Japan *HONDA* also showed great mobility and even can help people with some housework[3], [4]. Bio-robots *Cassie* of *Agility Robotics*, which mimics the ostrich, are able to walk in unstructured environment[5], [6]. In 2019, *Agility Robotics* developed *Cassie's* second-generation robot *Digit*, which can be used to transport express[7]. The classic two-wheeled robot *Segway* is used as a vehicle and a general robot development platform[8], [9]. And *uBot* robot was built by mounting two robot arms on two wheels[10], [11].

These robots are either foot-mounted or wheeled, and although they have achieved quite good achievements in their own fields, they cannot integrate the advantages of both. For example, although the foot robot has a good obstacle surmounting performance, it has lower moving efficiency and speed on the flat road surface. In contrast, the wheeled robot has faster moving speed and is more efficiency, but has poor adaptability in complex pavement. Therefore, it is necessary to develop a new legged-wheeled robot to combine the advantages of both, so that the robot can move quickly on the flat road with wheels and enhance its robust with its feet in an unstructured environment. And because the factories and homes built for human, and there are many narrow passageways, stairs, steps, and debris, therefore we designed the bipedal humanoid type legged-wheeled robot *SR600*, shown as Fig.1. The system presented in[12] is the most similar design to the *SR600* robot. It combines wheels and legs efficiently, but due to its size, it is unfit for human habitation. The *SR600* can adapt to the environment of interaction with people or dense crowds, such as home and airport.

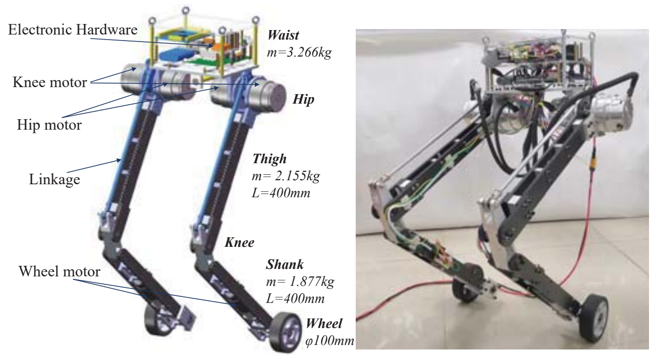

Fig. 1. Left:The solidworks model of SR600 and its components properties; right: SR600 prototype.

The *SR600* refers to the design and control methods of *Ascento*[13], [14], but *Ascento* overcomes obstacles by jumping. During the jumping process, the robot will cause a large bump to the carried load, which causes the robot not able to carry fragile items such as glass, ceramics, non-closed liquid, etc. And *Ascento* needs a large acceleration and deceleration working space to overcome obstacles, and it is impossible to continuously overcome obstacles. At the same time, *SR600* also refers to the control method of *Golem Krang*[15]–[17], which uses the mechanical structure properties of the robot to enhance the navigation of the robot, and controls the dynamic balance of the robot according to the relative inclination of the center of gravity of the robot. This paper introduces a ROS-Gazebo based simulation of variable height dynamic balance of a bipedal legged-wheeled robot *SR600*, and its simple experimental verification.

The remained of this paper is organized as fellows. Section II includes the mechanical structure in the ROS-Gazebo simulation and the derivation of the mathematical model of the robot. Section III describes the control method of the robot,

[1]Tangyou Liu, Chao Zhang, Shuang Song are with School of Mechanical Engineering and Automation, Harbin Institute of Technology(Shenzhen), Shenzhen, China, 518055.

[2]Max Q.-H. Meng is with Department of Electronic Engineering, the Chinese University of Hong Kong, Hong Kong, China, and affiliated with the State Key Laboratory of Robotics and Systems (HIT), Harbin Institute of Technology, China.

*Corresponding author: Shuang Song, mail: songshuang@hit.edu.cn

978-1-7281-6321-5/19//$31.00 ©2019 IEEE

which mainly includes the derivation of the wheel dynamic balance control and the variable height control method. Then in Section IV, the results of Section III will be verified in Gazebo and a simple prototype experiment will be carried out. Finally, future work and conclusions will be discussed in Section V.

II. MECHANICAL MODEL

A. Mechanism

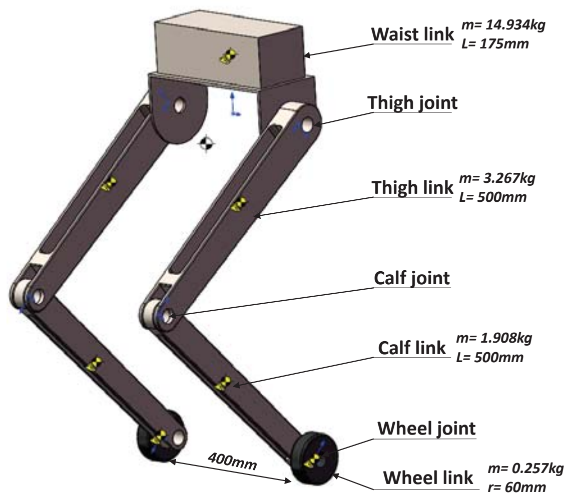

Fig. 2. A simplified robot model for simulation.

The system design of the robot is described in detail in another article. This paper mainly introduces the simplified structure of the robot and its URDF model for ROS-Gazebo simulation. The simplified model and related parameters are shown in Fig.2. The 14kg waist is to simulate the load capacity of the robot so that an end effector such as a robot arm or humanoid body can be installed in the future.

After establishing the relevant reference coordinate system and axis in SolidWorks, the URDF model is exported by the sw_urdf_exporter tool. The assembly relationship of each component is shown in Fig.3. Since the left and right legs are synchronized in the case of changing height in this paper. And in the subsequent joint constraint relationship derivation, we keep the top surface of the robot always in the equilibrium position. Therefor, the IMU can be directly installed on the top surface of the waist link.

B. Modeling

The principle of the traditional inverted pendulum balance is to achieve dynamic balance by oscillating the center of mass of the inverted pendulum in an equilibrium position by the movement of the chassis[18]. The robot in this paper wants to maintain the balance while changing the height, which is a dynamic process. Therefore, the main purpose of this paper is to find a way to maintain the center of mass(COM) of robot body always on the axis AF during the height of the robot is being changed. The axis AF is vertical ground and through the

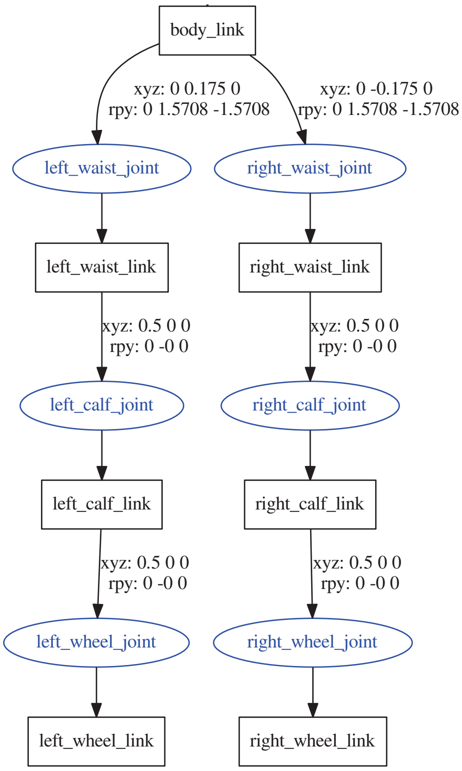

Fig. 3. Links relations and positions description of Urdf model.

axis of the center of the two-wheel axis, as shown in Fig.4. And we call this situation obeys the constraint of the center of mass(COCOM).

We establish the coordinates according to the rules of coordinate establishment of D-H parameter method, as shown in Fig.4. According to the geometric meaning represented by the D-H parameter, the corresponding parameters can be observed from the figure, as shown in Table.I[19].

TABLE I
D-H PARAMETERS OF THE ROBOT

i	a_i(mm)	α_i (°)	d_i(mm)	θ_i (°)	initial(°)	range(°)
1	L_1	0	0	θ_1	37	0~180
2	L_2	0	0	θ_2	140	15~165
3	L_3	0	0	θ_3	−87	−120~120

In order to obtain the COCOM, we need to figure out the position of the center of mass of the robot body.

According to the homogeneous transformation matrix:

$$ {}^{i}_{i+1}T = \begin{bmatrix} Q_i & q_i \\ 0 & 1 \end{bmatrix} = \begin{bmatrix} \mathscr{C}_i & -\lambda_i S_i & \mu_i S_i & a_i \mathscr{C}_i \\ S_i & \lambda_i \mathscr{C}_i & -\mu_i \mathscr{C} & a_i S_i \\ 0 & \mu_i & \lambda_i & d_i \\ 0 & 0 & 0 & 1 \end{bmatrix} \tag{1} $$

where ${}^{i}_{i+1}T$ represents the position and attitude transformation matrix of frame i+1 with respect to frame i;q_i represents the position transformation matrix ; Q_i represents the attitude transformation matrix. $\mathscr{C}_i = \cos\theta_i$, $S_i = \sin\theta_i$, $\lambda_i = \cos\alpha_i$, $\mu_i = \sin\alpha_i$.

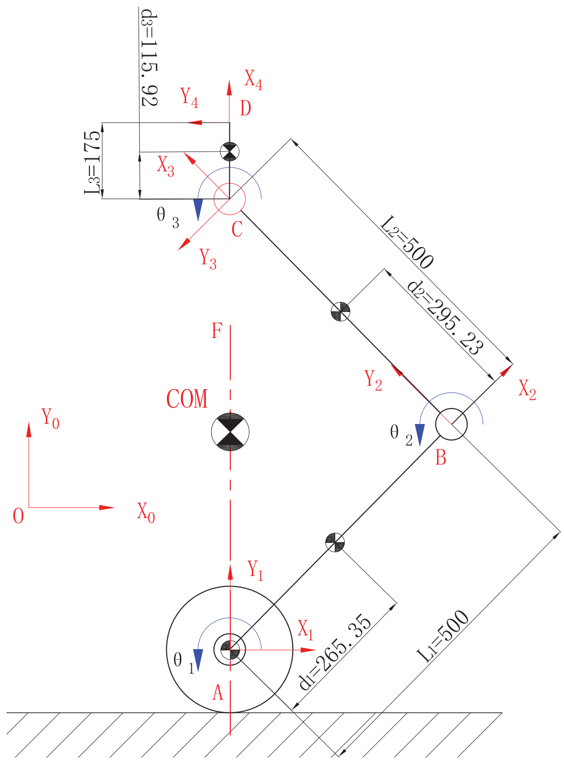

Fig. 4. The coordinates of the robot when modeling with DH parameter method. Where θ_i represent the relevant corner of joints, d_i represent the relative positions of the centroid of links, L_i represent the length of links, and COM represents the center of mass of the robot body.

We can get the position of the waist as fellow.

$$r_{14} = [L_1c_1 + L_2c_{12} + L_3c_{123} \quad L_1s_1 + L_2s_{12} + L_3s_{123} \quad 0] \quad (2)$$

where $c_1 = \cos\theta_1$; $s_1 = \sin\theta_1$; $c_{12} = \cos(\theta_1+\theta_2)$; $s_{12} = \sin(\theta_1+\theta_2)$; $c_{123} = \cos(\theta_1+\theta_2+\theta_3)$; $s_{123} = \sin(\theta_1+\theta_2+\theta_3)$.

Then according to the vector conversion relationship:

$$C_i = r_{1,i} + Q_i r_{i,C_i} \quad (3)$$

where C_i is the position vector of the link i under coordinate system 1; $r_{1,i}$ is the position vector of the origin of the coordinate i under the coordinate system 1; r_{i,C_i} represents the position vector of the centroid of the component i relative to the origin of the coordinate system i under the coordinate system i.

We can get the following equations:

$$C_2 = \begin{bmatrix} d_1c_1 & d_1s_1 & 0 \end{bmatrix}' \quad (4)$$

$$C_3 = [d_2c_{12} + L_1c_1 \quad d_2s_{12} + L_1s_1 \quad 0]' \quad (5)$$

$$C_4 = [L_2c_{12} + L_1c_1 + d_3c_{123} \quad L_2S_{12} + L_1s_1 + d_3s_{123} \quad 0]' \quad (6)$$

$$C_m = \begin{bmatrix} (2d_1m_2c_1 + 2m_3(d_2c_{12} + L_1c_1) + \\ m_4(L_2c_{12} + L_1c_1 + d_3c_{123}))/m\_b \\ (2d_1m_2s_1 + 2m_3(d_2s_{12} + L_1s_1) + \\ m_4(L_2s_{12} + L_1s_1 + d_3s_{123}))/m\_b \\ 0 \end{bmatrix} \quad (7)$$

where C_2, C_3, C_4, C_m respectively indicate the position of the COM of calf, thigh, waist and robot body under the coordinate system 1; m_2, m_3, m_4 are the mass of calf, thigh and waist respectively; $m\_b = 2m_2 + 2m_3 + m_4$; '′' indicates the transpose of the matrix.

In order to keep the center of mass of the robot body in the equilibrium position, the following constraint equation (8) is established.

$$\begin{aligned} &(2d_1m_2c_1 + 2m_3(d_2c_{12} + L_1c_1) + \\ &m_4(L_2c_{12} + L_1c_1 + d_3c_{123}))/m\_b = 0 \end{aligned} \quad (8)$$

And the height h of the robot is represented by the y coordinate of the top surface of waist, as shown in equation (9).

$$L_1s_1 + L_2s_{12} + L_3s_{123} = \mathrm{h} \quad (9)$$

Since we also want to keep the waist parallel to the ground while maintaining balance, we have established an additional constraint equation (10).

$$\theta_1 + \theta_2 + \theta_3 = pi/2 \quad (10)$$

According to (7), (8) and (9), and taking the relevant parameter values, the function relationship of θ_1, θ_2 and θ_3 with h under the COCOM constraint condition is obtained respectively.

$$\theta_1 = \arcsin\frac{-16A + \sqrt{400A^2 + 81}}{9} \quad (11)$$

$$\theta_3 = \arccos\frac{25A - \sqrt{400A^2 + 81}}{9} \quad (12)$$

$$\theta_2 = \pi/2 - \theta_1 - \theta_3 \quad (13)$$

where $A = \frac{h - L_3}{L_1} > 0$; $0 < \theta_1 < \frac{pi}{2}$; $-\frac{pi}{2} < \theta_3 < 0$.

III. CONTROL

A bipedal wheeled robot is inherently unstable. Thus, dedicated control strategies are required not only for changing height, but even standing still and driving.

A. Dynamic Balance Control

In order to achieve a height change of the robot while maintaining balance, a reliable balance control algorithm is required. But since the focus of this research is to study how robots can change heights, PID controller is used in dynamic balance control. Research on model-based LQR control algorithms will be carried out in future work [20]. PID controller is based on the tilt angle error, which is defined as the difference between the set point (0) and the measured tilt angle. The control law is defined by the equation(14).

$$u(t) = K_p\left(e(t) + \frac{1}{T_i}\int_0^t e(\tau)d\tau + T_d\frac{de(t)}{dt}\right) \quad (14)$$

Equation (14) is composed by the following three terms: proportional, integral and derivative. The proportional action is a gain value (Kp) multiplied by the error function. With a high value of K the steady state error decreases and accelerates the response of the system to the defined set point, however it can also raise the oscillations within the output signal[21]. On the other hand, the integral action eliminates the steady state error through the iterative accumulation of past errors. Finally, the derivative action reduces the oscillations in the output resulting from the proportional and integral action. With the derivative gain value, the stability of the closed response is improved[21].

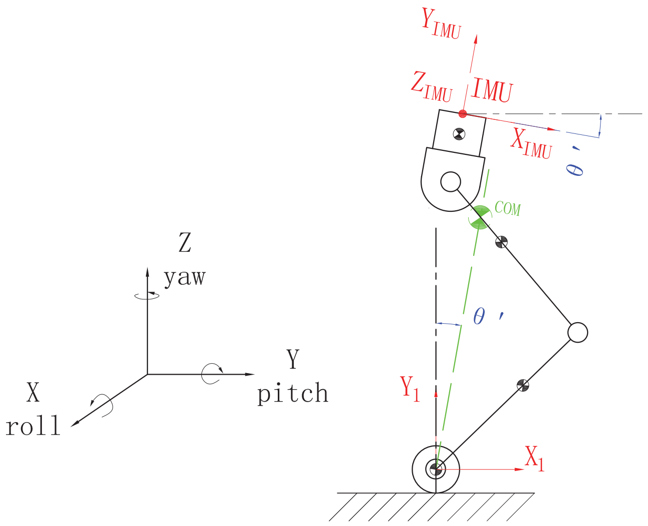

Fig. 5. IMU is placed on the top of the waist link, and the θ is the tilt Angle of robot. The angle θ' measured by IMU is equal to θ.

Since the equation (10) makes the top surface of waist link always parallel to the ground surface when the robot is in the equilibrium position, the IMU can be placed directly on the top surface of the waist, as shown in Fig.5. The yaw axis angle θ' is obtained by IMU, which in Gazebo is relative angle, and the initial deviation angle of each axis is 0. Therefore, the θ' read by IMU can be used as tilt Angle of PID controller in real time.

B. Change Height Control

In the study of optimized planning and control for dynamically stable robots under vertical obstacles based on *Golem Krang robot*, Kasemist et al. achieved vertical obstacle avoidance by controlling the upper body of the robot to tilt a certain angle[16]. But in their research, the robot needs a large moving space to prepare for the early stage when implementing vertical obstacle avoidance. The research in this paper, thanks to the design of the robot structure, enables the robot to achieve the height change while keeping the two wheels in place, so that the robot can realize vertical obstacle avoidance in a very small moving space.

The research on the robot height control method is to find a way to enable the robot to achieve vertical obstacle avoidance in the future protoptyes. Due to the structural limitations of the robot and the avoidance of singularities, the workspace of the robot height is limited to between 500mm and 1100mm. And through matlab we can get the relationship curves between θ_i and height, as shown in Fig.6, and we can find them are

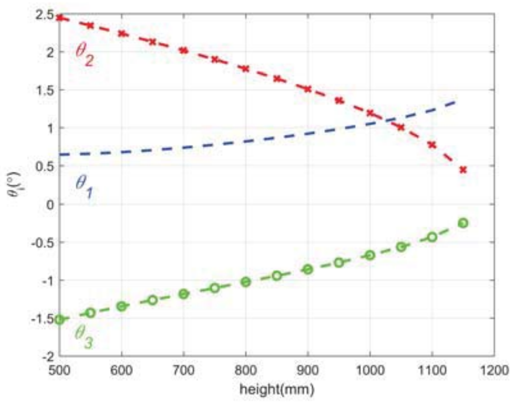

Fig. 6. The relationship between joint angles θ_i and height. Where theta$_i$ corresponds to θ_i in Fig.4, and respectively represent the angle between the lower leg of the robot and the ground, the angle of the knee joint, and the angle of the waist joint.

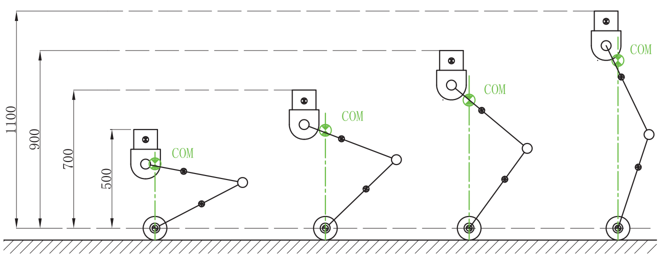

Fig. 7. Dynamic balance diagram of robot with variable height. The COM is always on the green axis, and the number is the height which means the distance of top surface to the wheel center.

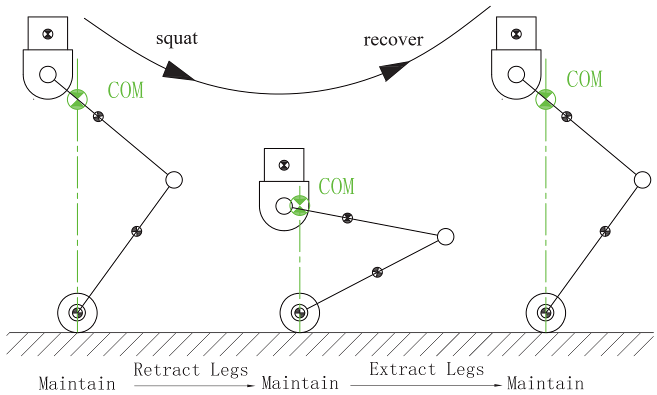

Fig. 8. The discrete phases of the squatting and recovering.

continue. In addition, we used the robotic toolbox of matlab to generate a simple three-dimensional model, and obtained the curve of the robot's centroid by rotating the joints according to the above constraint, which meets the COCOM.

When the height that the robot expects to reach is input, the corresponding joint angles will be calculated by equations (10), (11) and (12). Then joints will be controlled to go to the corresponding positions. Due to COCOM, COM is always near the axis of the equilibrium position when the joint angle is rotating. The balance control of the robot adopts a PID controller and it has certain robustness. At the same time, when the joint angle of the robot is rotated slowly, no large disturbance is generated. Therefore, the robot can still maintain balance when changing the height. The schematic diagram of the robot changes the height is shown in Fig.7, and the center of mass will always be in equilibrium when changing the height of the robot. Finally the robot can realize the movement states of squatting, maintaining balance under the constant height and recovering to the original position by retracting legs and extracting legs, as shown in Fig.8.

IV. SIMULATION & EXPERIMENT

Due to the complex structure of the prototype, calculating the centroid, calculating the principal moment, and establishing the math model of SR600 require a large amount of work, and the purpose of this paper is to verify the feasibility of the method of changing the height. Therefore, this paper mainly based on the simplified model for simulation experiments. On the prototype, only a simple verification was performed at several heights to show the feasibility of the proposed method.

According to the actual situation of the prototype, we have made some settings and assumptions about the simulation environment, and make the simulation environment as simple as possible without affecting the reliability of the simulation results.

(1) Since the joint motor in the prototype is QDD-6010-64 of *INNFOS*, and the rated torque is 40.55Nm. The motor used in the wheels are *RoboMaster* RM35 DC brush motor, driven by a 24V battery, with a torque factor of 353.117 g.cm/A and a rotational speed constant of 274 rpm/V. Through the derivation of the dynamic model of the robot, the motor can fully meet the torque required for the rotation of the joints. Therefore, the torque we set in the simulation should fully meet the requirements of the joint movement of the robot.

(2) Now the control of changing the height is only concerned. We use position control in the waist and calf joints, and do not consider the dynamic influence factors introduced by the rotation of waist and calf links. We also assumed that the position control of ROS-Gazebo is reliable, and the joint angles of the robot can reach the corresponding positions after being controlled.

(3) The friction between the wheel and the ground is sufficient, and the wheels do not slide relative to the ground.

The robot is simulated in ROS-Gazebo as shown in Fig.9. The two-wheel control directly utilizes the ROS differential controller plugin, and also used the IMU plugin to measure the corner and speed for dynamic balance. In order to adjust the parameters, the dynamic parameter plugin *rqt_reconfigue_param_rqt* is added in the ROS-Gazebo simulation environment. Fig.10 shows the used ROS nodes and topics in simulation. In the simulation environment, we simulated the movement of the robot to squat, maintain and recover, and used the *rqt_plot* tool to collect the joint angles and the IMU data of the robot, as shown in Fig.11, which shows a running cycle data of the robot. In the figure, *Joint_1, joint_2, joint_3, and joint_4* correspond to the left hip joint, the right hip joint, the left knee joint, and the right knee joint of the robot, respectively. And the IMU data shows that the robot is

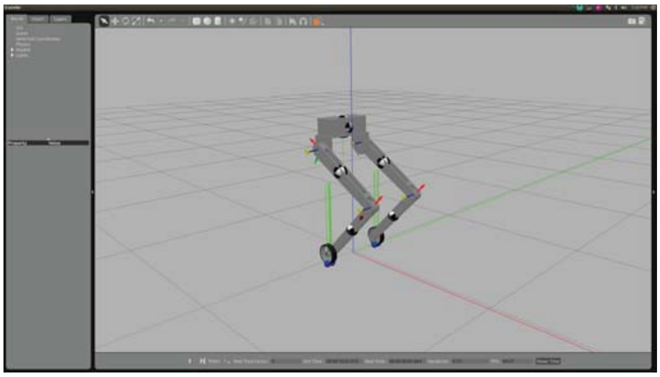

Fig. 9. ROS-Gazebo simulation environment of bipedal wheeled robot.

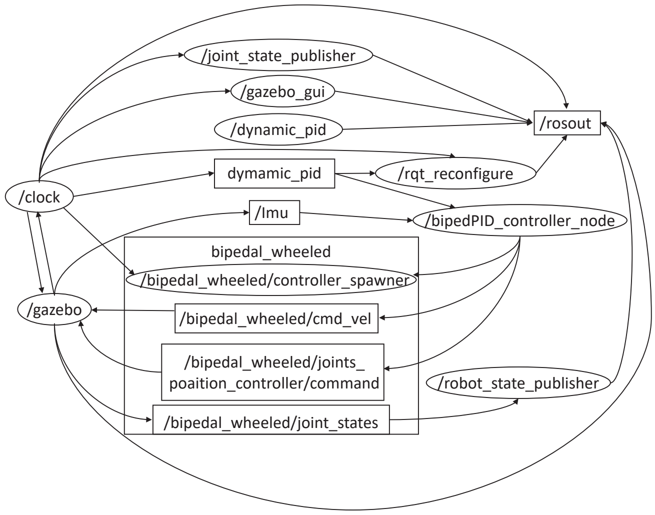

Fig. 10. The used ROS nodes and topics in simulation

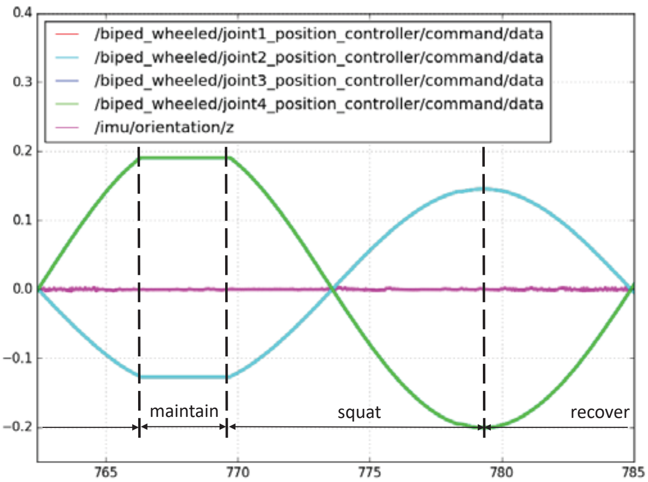

Fig. 11. Joint angles and IMU data of the robot during one operating cycle.

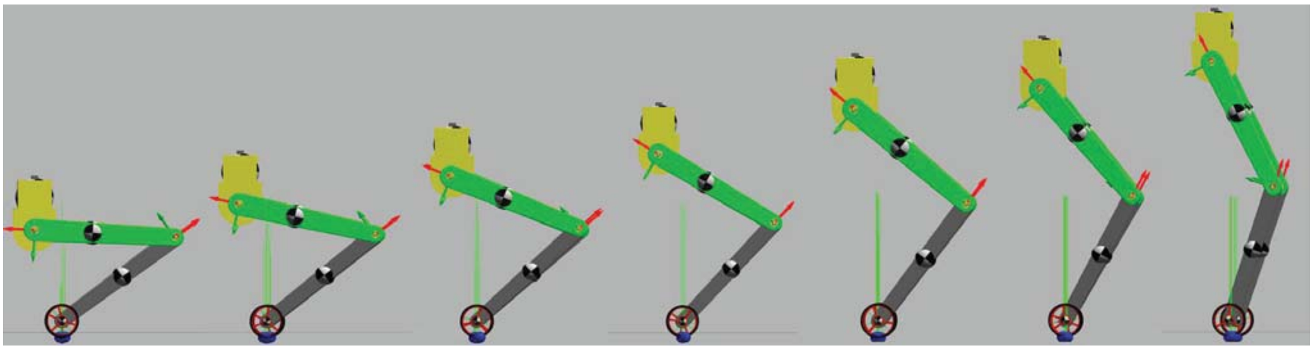

Fig. 12. The simulation results in the range of 500mm to 1100mm

always balanced during the operating cycle. And Fig.12 shows the robot's operating state in the simulation environment in the range of 500mm to 1100mm.

According to the above simulation results, we conducted a simple verification on the prototype, as shown in Fig.13. The result shows that the purposed method in this paper is feasible. The much more detailed control processes and experiments will be further optimized on the basis of detailed analysis and modeling in the future.

V. CONCLUSION

This paper introduced a method for changing the height when the bipedal wheeled robot is in balance, then simulated it by constructing a simple ROS-Gazebo simulation environment and carried some simple experiments of the method on the prototype to verify its feasibility. By constraining the center of mass to the axis that perpendicular to the ground and passing through the center of the two-wheel, the bipedal wheeled robot can change the height while maintaining dynamic balance. This will allow the robot to have a larger vertical operating space. The waist can be equipped with an end effector such as a robot arm in the future, which will make the SR600 robot as a universal platform and can achieve friendly interaction with humans. In the future, we will carry out more detailed experimental verifications on the prototype, and the research on control algorithms that through changing height to avoid vertical obstacles will be carried out. And the much more robust stabilization algorithm will be applied to the robot, such as LQR, Fuzzy and H∞.

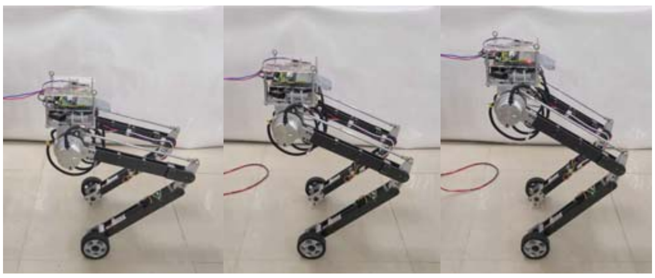

Height = 500mm Height = 600mm Height = 700mm

Fig. 13. The experiment on the prototype

REFERENCES

[1] Atlas. Accessed: 05.09.2019. [Online]. Available: https://www.boston-dynamics.com /atlas.

[2] Boston Dynamics' Atlas Robot Can Do Parkour. Accessed: 05.09.2019. [Online]. Available: https://www.youtube.com/watch?v=hSjKoEva5bg.

[3] J. Chestnutt, M. Lau, G. Cheung, J. Kuffner, J. Hodgins, and T. Kanade, "Footstep planning for the honda asimo humanoid," pp. 629–634, 2005.

[4] Y. Sakagami, R. Watanabe, C. Aoyama, S. Matsunaga, N. Higaki, and K. Fujimura, "The intelligent asimo: System overview and integration," vol. 3, pp. 2478–2483, 2002.

[5] Cassie. Accessed: 05.09.2019. [Online]. Available: http://www.agility robo tics.com/ ?utm_source=robots.ieee.org#!cover.

[6] Cassie bipedal robot a platform for tackling locomotion challenges. Accessed: 05.09.2019. [Online]. Available: https://www.therobotreport .com/cassie-bipedal-robot-a-platform-for-tackling-locomotion-challeng-es/.

[7] Agility Robotics Digit adds arms to Cassies bipedal design. Accessed: 05.09.2019. [Online]. Available: https://www.therobotreport.com/digit-agility-robotics-biped/.

[8] Segway. Accessed: 05.09.2019. [Online]. Available: http://www.segway.com/.

[9] H. G. Nguyen, J. Morrell, K. D. Mullens, A. B. Burmeister, S. Miles, N. Farrington, K. M. Thomas, and D. W. Gage, "Segway robotic mobility platform," vol. 5609, pp. 207–220, 2004.

[10] S. R. Kuindersma, E. Hannigan, D. Ruiken, and R. A. Grupen, "Dexterous mobility with the ubot-5 mobile manipulator," pp. 1–7, 2009.

[11] D. Ruiken, J. P. Cummings, U. R. Savaria, F. C. Sup, and R. A. Grupen, "ubot-7: A dynamically balancing mobile manipulator with series elastic actuators," pp. 676–682, 2017.

[12] Handle. Accessed: 05.09.2019. [Online]. Available: https://www.boston-dynamics.com/handle.

[13] Ascento. Accessed: 05.09.2019. [Online]. Available: https://www.ascen-to.ethz.ch.

[14] V. Klemm, A. Morra, C. Salzmann, F. Tschopp, K. Bodie, L. Gulich, N. Küng, D. Mannhart, C. Pfister, M. Vierneisel *et al.*, "Ascento: A two-wheeled jumping robot," pp. 7515–7521, 2019.

[15] M. Stilman, J. Wang, K. Teeyapan, and R. Marceau, "Optimized control strategies for wheeled humanoids and mobile manipulators," pp. 568–573, 2009.

[16] K. Teeyapan, J. Wang, T. Kunz, and M. Stilman, "Robot limbo: Optimized planning and control for dynamically stable robots under vertical obstacles," pp. 4519–4524, 2010.

[17] M. Stilman, J. Olson, and W. Gloss, "Golem krang: Dynamically stable humanoid robot for mobile manipulation," pp. 3304–3309, 2010.

[18] H. Simpson, *Dumb Robots*, 3rd ed, Ed. Springfield: UOS Press, 2004.

[19] B. Siciliano, L. Sciavicco, L. Villani, and G. Oriolo, *2009Robotics: Modelling, Planning, and Control*. New York: Springer.

[20] S. Wenxia and C. Wei, "Simulation and debugging of lqr control for two-wheeled self-balanced robot," pp. 2391–2395, Oct 2017.

[21] H. T. Astrom, K.J., *Control PID Avanzado*. Pearson Prentice Hall, Upper Saddle River, 2009.